Plasma-Induced Efficiency Enhancement in a Backward-Wave Oscillator

A. T. Lin and L. Chen[a]

Department of Physics, University of California, Los Angeles, Los Angeles, California 90024-1547

(Received 12 June 1989)

A dense background plasma is observed through computer simulation to reduce the phase velocity of the most unstable mode in a backward-wave oscillator which results in a strong efficiency enhancement. The relatively weak beam–backward-plasma-wave instability introduced by the rippled waveguide wall is found to exert minimal impact on the interaction efficiency.

PACS numbers: 52.60.+h, 52.65.+z

One of the very promising schemes for generating high-power microwave pulses is based on the interaction of a relativistic electron beam with the slow electromagnetic wave in a rippled-wall waveguide. During the last two decades relatively active experimental investigations[1-4] have been carried out to demonstrate the potential of this mechanism. Output power of 15 GW with 50% efficiency from a vacuum multisection Cherenkov generator has been reported.[5] Theoretical analyses[6-8] and particle simulations[8] have also been performed to evaluate the device performance.

The output power can be increased by raising the relativistic-electron-beam current to the extent that it is still well below the space-charge–limited current. To further increase the beam current, a background plasma must be employed to provide space-charge neutralization. Recently,[9] in experiments with a plasma-filled backward-wave oscillator (BWO), it was observed that the output power improved from about 60 (vacuum BWO) to 500 MW. This eightfold enhancement cannot be accounted for by the increased beam current alone. Some other mechanism must be occurring to explain this dramatic improvement. The improved BWO performance was attributed to the excitation of a beam–backward-plasma-wave instability. Kurilko, Kucherov, and Ostrovskii[7] have carried out a theoretical analysis of a plasma-filled BWO and shown that the gain can be enhanced by a factor of 5 from its vacuum value if the plasma frequency $\omega_p \simeq ck_0$ (k_0 is the ripple-wall wave number and c is the speed of light). However, the best experimental result[9] is operated with $\omega_p \simeq 0.2ck_0$. In this paper it will be shown that the excitation of the above-mentioned instability is highly unlikely. Furthermore, it will be illustrated that a dense background plasma tends to reduce the phase velocity of the most unstable BWO mode and cause the electrons to give up more energy to the wave.

To address the plasma effects on BWO efficiency, a particle-waveguide code[10] has been used, which follows the trajectories of a large number of electrons in time according to the relativistic equation of motion under the influence of the self-consistent, as well as the externally applied, electromagnetic fields.

The radial field structure is that of a TM_{01} mode of a constant-radius waveguide, but the radius is varied periodically along the axial direction. As a result, the cutoff frequency and the waveguide radius in the argument of the Bessel function are both varied accordingly. Periodic boundary conditions are assumed in the axial direction so that the nth-mode wave number is defined as $k_{zn}=2\pi n/L$, where L is the system length and is chosen to be $256\lambda_g$ (λ_g is the spatial grid size). The lowest 60 Fourier modes are followed in time through Maxwell's equation and 100 electrons per grid are employed. All three spatial and three velocity dimensions are followed but a strong axial magnetic field is imposed to restrict the electron-beam propagation along the axial direction. This simple model retains most of the essential physics in the interaction. The goal of this investigation is to elucidate the basic physics involved in the interaction. To simulate a real device, more realistic boundary conditions have to be imposed, such as the model employed in Ref. 8. The beam and rippled-waveguide parameters utilized in the experiment[9] are used in our simulation. The energy and current of the relativistic electron beam are, respectively, 640 kV and 2.5 kA. The rippled-wall waveguide is described by the following expression:

$$R_w = R_0(1+\epsilon \sin k_0 z)\,, \tag{1}$$

where $R_0=13.90\lambda_g$, $\lambda_g=0.104$ cm, and $k_0=k_{zn}$ for $n=16$ in our simulation system. The background plasma frequency ω_p is chosen to be $0.4\omega_c$ [$\omega_c=\mu_{01}c/R_0$, where μ_{0n} satisfies $J_0(\mu_{0n})=0$] which yields the best efficiency enhancement result in our simulation. All frequencies are normalized to ω_c. Both beam and plasma electrons are assumed to fill up uniformly the waveguide cross section up to $R=R_0(1-\epsilon)$. Initially, the beam and plasma velocity spreads along axial and transverse directions are taken to be 3% of the axial drift velocity of the beam. The electrostatic space-charge wave associated with the electron beam is a volume wave which is located in the source region. Therefore, regardless of the amount of beam current, it always requires a number of orthogonal vacuum modes (different μ_{0n}) to represent its radial profile. Thus one may have to resort to the use of the MAGIC code[8] to accurately describe the space-charge wave. In the situation of domination by the TM_{01} mode in the electromagnetic interaction (supported by experimental observations[9]), and using a large solid cross-section beam, the component of the space-charge wave

with the TM_{01} radial profile may be strongly coupled to the electromagnetic wave and becomes dominant. The dispersion relations of the decoupled beam slow space-charge wave ($\omega_b/\gamma^{3/2} \approx 0$, where γ is the relativistic energy parameter) and the electrostatic and the electromagnetic modes of a plasma-filled rippled waveguide are shown in Fig. 1(a) ($\epsilon = 0.1$). In the presence of the rippled wall, Floquet's theorem demands the solution to be periodic which results in two additional new features in comparison with that of a smooth-wall waveguide; that is, the existence of the backward-propagating plasma wave and the high-frequency TM slow wave.

To ensure that our simulation model contains all the essential modes with correct dispersion characteristics, the frequency spectrum of a rippled-wall waveguide filled with thermal plasma is simulated. The results are displayed as solid circles in Fig. 1(a) and they are in good agreement with the theoretical prediction. The frequency spectrum of a typical mode ($n = 11$) is exhibited in Fig. 1(b). In the simulation, the result of a negative-k_z mode is always the complex conjugate of the result of the positive-k_z mode so that a negative frequency from a positive-k_z mode is equivalent to a positive frequency from a negative-k_z mode. In ascending order, the various peaks in the spectrum correspond to backward plasma wave, forward plasma wave, slow TM wave, and fast TM wave. The last mode ($v_{ph} > c$) plays no role in microwave emission due to its inability to interact with the relativistic electron beam. Under the condition $\omega_p/\omega_c < \beta_b \gamma_0$ ($\beta_b = V_b/c$), which is satisfied in our simulation, the conventional beam-forward-plasma-wave instability will not be excited, but from the dispersion curve the beam line will definitely intersect the backward branch of the plasma wave. It will be shown later that this interaction is relatively weak and plays no role in enhancing the efficiency.

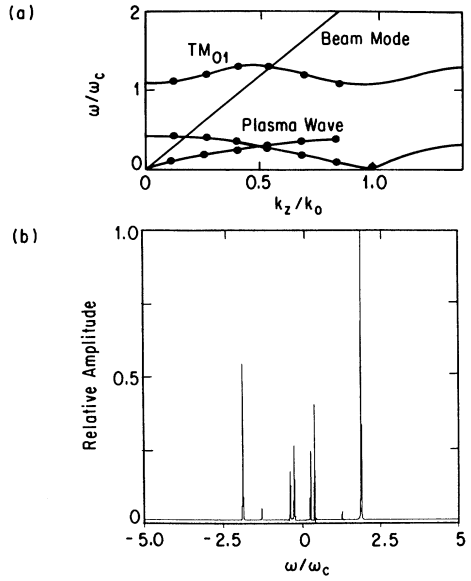

FIG. 1. The propagation characteristics of a plasma-filled rippled waveguide: (a) the dispersion relation including the electromagnetic and plasma waves, solid circles are the results from simulation; (b) the frequency spectrum of mode 11 ($k_z c = 1.55\omega_c$).

The microwave generation from a vacuum BWO is simulated first. Based on the coupling provided by the boundary condition that the tangential component of the electric field vanishes at the ripple wall, the dispersion relation can be obtained as[11]

$$D_0 = \frac{\epsilon^2}{4} J_0'(\lambda_0)\left[J_0'(\lambda_1)\frac{\beta_1}{D_1} + J_0'(\lambda_{-1})\frac{\beta_{-1}}{D_{-1}}\right], \quad (2)$$

where

$$\beta_{\pm 1} = \left(\frac{k_{z,\pm 1} \pm k_0/F_{\pm 1}}{k_{z0}}\right)\left(\frac{k_{z0} \mp k_0/F_0}{k_{z,\pm 1}}\right),$$

$$D_s = J_0(\lambda_s)/\lambda_s, \quad \lambda_s = \Gamma_s R_0,$$

$$F_s = 1 - \frac{\omega^2}{c^2 k_{zs}^2}, \quad k_{zs} = k_z + s k_0,$$

and

$$\Gamma_s^2 = -k_{zs}^2 F_s\left[1 - \frac{\omega_p^2}{\omega^2} - \frac{\omega_b^2}{\gamma^3(\omega - k_{zs}V_b)^2}\right]. \quad (3)$$

According to the theoretical prediction, the beam mode in the zeroth-order Brillouin zone ($\omega_0 \approx k_{z0}V_b$) should be coupled with the TM waveguide mode in the first-order Brillouin zone [$\omega_0 = (\omega_c^2 + k_{z,-1}^2 c^2)^{1/2}$] and grow together with the same frequency ω_0. In the limit of small ϵ and a solid cold beam the perturbation on ω_0 can be approximated by

$$\delta\omega = i\omega_0 \frac{\epsilon}{2}\mu_{01}\left|\frac{\beta_1}{C_0 C_1}\right|^{1/2}, \quad (4)$$

where $C_s = \omega_0 \partial\lambda_s/\partial\omega_0$ and Eq. (4) is valid if $|\delta\omega| < |\omega_0 - k_{z0}V_b|$.

The wave-energy time evolutions of the most unstable modes are shown in Fig. 2(a). Their respective frequency spectra are given in Fig. 2(b), which confirms that both are oscillating at $\omega_0 = 1.26\omega_c$ and the wave number of the beam mode is $k_{z0}c = 1.41\omega_c$ ($n = 10$) whereas that of the TM mode is $k_{z,-1}c = -0.85\omega_c$ ($n = -6$). The temporal growth rate estimated from the simulation is $0.014\omega_c$, which is below the theoretical prediction $\delta\omega = 0.019\omega_c$ [Eq. (4)]. This discrepancy could be primarily due to the fact that the simulation beam has an initial 3% thermal spread. For comparison, a simulation run with 5% thermal spread has also been carried out and the resulting growth rate is lower ($\delta\omega = 0.012\omega_c$). The radiation energy is concentrated mostly in the TM fast wave ($s = -1$) as is evident from Fig. 2(a). The simulation results also reveal that mode 6 has an earlier start and mode 10 starts to grow when mode 6 attains an amplitude which satisfies the equilibrium mode energy

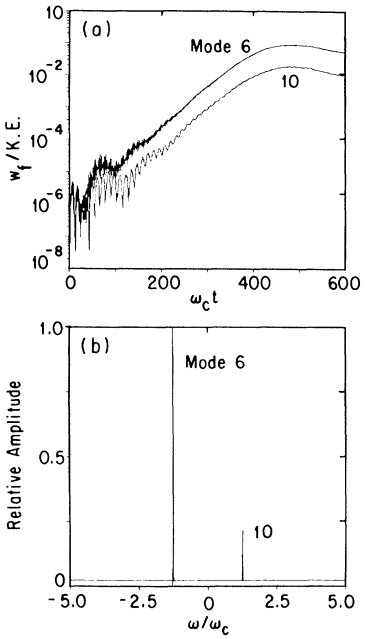

FIG. 2. Simulation results of a vacuum backward-wave oscillator: (a) the time evolution of wave energy of unstable modes and (b) their frequency spectra.

distribution in the presence of rippled-wall coupling. These two modes exponentiate with the same growth rate and saturate at the same time, which is strong evidence of mode coupling.

The saturation mechanism of a BWO is due to trapping of the electrons by the axial electric field of the beam mode, which has been clearly demonstrated in the beam phase diagram at $\omega_c t = 500$ [Fig. 3(a)]. At the time of saturation, the mean beam electron velocity is on the average slowed down to the phase velocity of the slow wave. The efficiency of a BWO can be roughly expressed as $\eta = (\gamma_0 - \gamma_{ph})/(\gamma_0 - 1)$, where γ_0 is the initial beam energy and $\gamma_{ph} = [1 - (v_{ph}/c)^2]^{1/2}$ corresponds to the energy of a particle moving at the phase velocity of the wave.[12] Therefore the efficiency of a BWO depends on the difference between the beam drifting velocity ($V_b \simeq 0.9c$) and the phase velocity of the beam mode (v_{ph}). In the case we simulated $v_{ph} \simeq 0.894c$, which results in only about 6% efficiency for the vacuum BWO.

The simulation results of the plasma-filled BWO are shown in Figs. 3 and 4. The beam axial velocity versus distance plotted at the time of saturation ($\omega_c t = 520$) shows that the trapping width is greatly enhanced in the presence of the plasma [Fig. 3(b)] ($\omega_p \cong 0.4\omega_c$) and the efficiency is increased to about 36%. The efficiency is estimated from the expression $\eta = (\gamma_0 - \gamma_f)/(\gamma_0 - 1)$, where γ_f is the minimum beam energy in the time evolution of beam energy [Fig. 3(c)]. After saturation the wave and electron energies are observed to slosh back and forth if the simulation is run longer. In this case the unstable coupled modes are mode 5 and mode 11 which

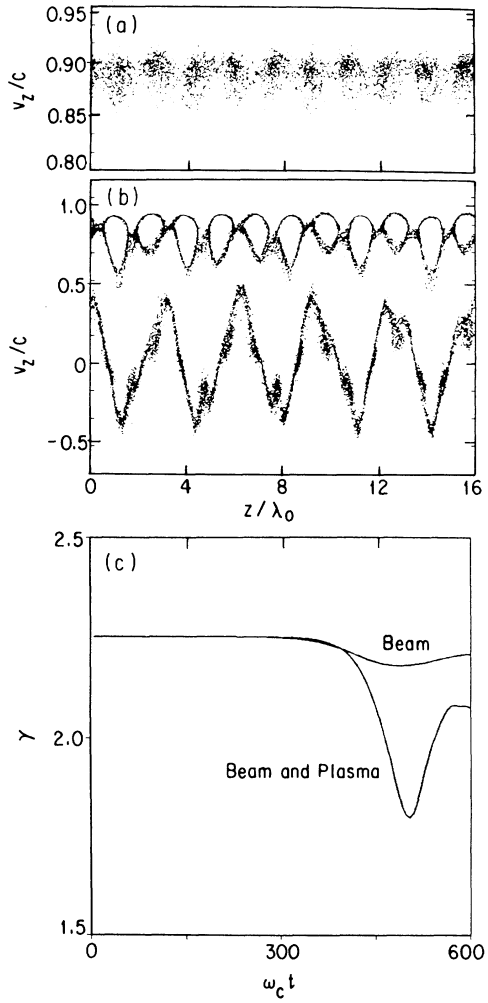

FIG. 3. Electron axial velocity vs distance for (a) vacuum BWO at $\omega_c t = 500$ and for (b) plasma-filled BWO at $\omega_c t = 520$; (c) the time evolution of beam energy for both cases.

strongly perturb, respectively, the plasma and beam phase spaces. This is because mode 11 is in resonance with the beam drift motion whereas neither mode is in resonance with plasma electrons, and hence the plasma responds passively to the axial electric field of the unstable modes according to their amplitudes. The fact that this strong plasma perturbation is not due to the beam-plasma interaction is further supported by the frequency-spectrum analysis [Fig. 4(b)] which shows no evidence of a plasma-oscillation component. The effects of background plasma tend to slightly increase the growth rate ($0.015\omega_c$) as well as the real frequency ($1.285\omega_c$) of the unstable modes [Fig. 4(a)], in agreement with the results of Ref. 7. At the same time the beam-mode axial wave number has been shifted to 11 which results in lower phase velocity ($v_{ph} \cong 0.83c$) and thus increases the efficiency by a factor of 6 [Fig. 3(c)]. The influence of a plasma on the performance of a BWO

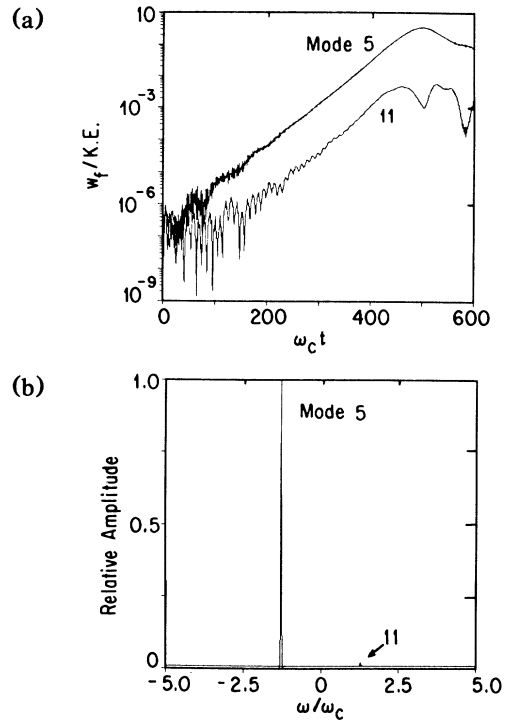

FIG. 4. Simulation results of a plasma-filled BWO: (a) the time evolution of wave energy of unstable electromagnetic modes and (b) their frequency spectra.

becomes significant only if ω_p is a major fraction of ω_c such that the mode phase velocity is substantially modified. The full plasma effect can only be evaluated from solving the original dispersion relation [Eq. (2)] or performing computer simulations.

In analogy to a vacuum BWO the rippled wall should also provide the coupling for the beam slow space-charge wave and the backward plasma wave. However, simulation results reveal no trace of this interaction, which may be attributed to the fact that the strong BWO interaction overwhelms the weak beam-plasma interaction. To elucidate this uncertainty, the latter is isolated by using the electrostatic approximation, both in simulation and theoretical analysis. Both results show that the growth rate of the beam-backward-plasma-wave interaction is more than an order of magnitude smaller than that of the vacuum BWO, and the impact of this mode on the efficiency of a BWO will be minimal. Therefore, we arrive at the conclusion that the wave-phase-velocity retardation induced by background plasma is a more plausible explanation for the efficiency enhancement observed in experiments.[9] However, the plasma-induced changes in the beam density and velocity are not included in the simulation. In order to single out the absolute mechanism responsible for the observed efficiency enhancement, a more realistic simulation has to be performed.

This work was supported by the Air Force Office of Scientific Research under Grant No. AFOSR 88-0027, the National Science Foundation under Contract No. ECS86-03644, and the San Diego Supercomputing Center.

[a]Permanent address: Princeton Plasma Physics Laboratory, Princeton, NJ 08544.

[1]Y. Carmel, J. Ivers, R. E. Kribel, and J. Nation, Phys. Rev. Lett. **33**, 1278 (1974).

[2]Y. V. Tkach *et al.*, Fiz. Plazmy **1**, 81 (1975) [Sov. J. Plasma Phys. **1**, 43 (1975)].

[3]V. L. Bratman, G. G. Denisov, S. D. Korovin, V. V. Rostov, S. D. Dolevin, and A. F. Yakushev, Pis'ma Zh. Tekh. Phys. **9**, 617 (1983) [Sov. Tech. Phys. Lett. **9**, 266 (1983)].

[4]Y. Carmel, V. L. Granatstein, and A. Gover, Phys. Rev. Lett. **51**, 566 (1983).

[5]S. P. Bugaev *et al.*, Sov. J. Comm. Tech. Electron. **32**, 79 (1987).

[6]A. Bromborsky and B. Ruth, IEEE Trans. Microwave Theory Tech. **32**, 600 (1984).

[7]V. I. Kurilko, V. I. Kucherov, and A. D. Ostrovskii, Zh. Tekh. Fiz. **51**, 1415 (1981) [Sov. Phys. Tech. Phys. **26**, 812 (1981)].

[8]J. A. Swegle, J. W. Poukey, and G. T. Leifeste, Phys. Fluids **28**, 2882 (1985).

[9]Y. Carmel, K. Minami, R. A. Kehs, W. W. Destler, V. L. Granatstein, D. Abe, and W. L. Lou, Phys. Rev. Lett. **62**, 2389 (1989).

[10]M. Caplan, Ph.D. dissertation, University of California at Los Angeles, UCLA Report No. PPG-963, 1986 (unpublished).

[11]The detailed derivation of the dispersion relation will be contained in a future publication.

[12]T. Kwan, J. M. Dawson, and A. T. Lin, Phys. Fluids **20**, 581 (1977).